PDZ interaction site in ephrinB2 is required for the remodeling of lymphatic vasculature

Taija Mäkinen,[1] Ralf H. Adams,[2] John Bailey,[1] Qiang Lu,[3] Andrew Ziemiecki,[4] Kari Alitalo,[5] Rüdiger Klein,[1,6] and George A. Wilkinson[1]

[1]Department of Molecular Neurobiology, Max-Planck Institute of Neurobiology, 82152 Munich-Martinsried, Germany; [2]Cancer Research UK-London Research Institute, London WC2A 3PX, United Kingdom; [3]Division of Neurosciences, Beckman Research Institute of City of Hope, Duarte, California 91010, USA; [4]Department of Clinical Research, Faculty of Medicine, University of Bern, 3004 Bern, Switzerland; [5]Molecular/Cancer Biology Laboratory, Biomedicum Helsinki, University of Helsinki, 00014 Helsinki, Finland

The transmembrane ligand ephrinB2 and its cognate Eph receptor tyrosine kinases are important regulators of embryonic blood vascular morphogenesis. However, the molecular mechanisms required for ephrinB2 transduced cellular signaling in vivo have not been characterized. To address this question, we generated two sets of knock-in mice: *ephrinB2*$^{\Delta V}$ mice expressed ephrinB2 lacking the C-terminal PDZ interaction site, and *ephrinB2*^{5F} mice expressed ephrinB2 in which the five conserved tyrosine residues were replaced by phenylalanine to disrupt phosphotyrosine-dependent signaling events. Our analysis revealed that the homozygous mutant mice survived the requirement of ephrinB2 in embryonic blood vascular remodeling. However, *ephrinB2*$^{\Delta V/\Delta V}$ mice exhibited major lymphatic defects, including a failure to remodel their primary lymphatic capillary plexus into a hierarchical vessel network, hyperplasia, and lack of luminal valve formation. Unexpectedly, *ephrinB2*$^{5F/5F}$ mice displayed only a mild lymphatic phenotype. Our studies define ephrinB2 as an essential regulator of lymphatic development and indicate that interactions with PDZ domain effectors are required to mediate its functions.

[*Keywords*: PDZ; ephrin; Eph; lymphatic valve; collecting lymphatic vessel; smooth muscle]

Supplemental material is available at http://www.genesdev.org.

Received June 25, 2004; revised version accepted December 3, 2004.

The vertebrate circulatory system is composed of blood and lymphatic vessels, which are closely related in terms of their origin, morphogenesis, and molecular cues regulating their development and growth. However, the two vascular systems have different fine structures, serve distinct roles, and require strict separation (Rossant and Howard 2002; Oliver 2004). During embryonic development, blood vessels originate from mesodermally derived endothelial precursors during a process called vasculogenesis. These vessels grow and remodel into a mature network of hierarchically organized vessels both by the regression of vessels and by angiogenesis, which consists of sprouting, splitting, and fusion of pre-existing vessels. Lymphatic vessels appear to originate from a subset of venous endothelial cells, which commit to the lymphatic endothelial cell (LEC) lineage and sprout from the major veins in the jugular and perimesonephric area to form lymphatic sacs, from which the vessels subsequently grow by centrifugal sprouting (for review, see Alitalo and Carmeliet 2002; Oliver and Detmar 2002). Similarly to the blood vasculature, the lymphatic system undergoes maturation and remodeling, although here the process is less well understood (see below).

The major functions of the lymphatic vasculature are to maintain tissue fluid balance and to provide immune surveillance and a route for fat absorption in the gut. The unidirectional lymph flow recovers extravasated tissue fluid from the periphery by blind-ended lymphatic capillaries, which drain into larger collecting lymphatic vessels and return the lymph to the cardiovascular system via the thoracic duct, which empties directly into the left subclavian vein. Unlike blood vessels, the lymphatic capillaries have discontinuous basement membrane; they form loose intercellular junctions, lack pericyte coverage, and are therefore highly permeable to large macromolecules. In contrast, larger collecting lymphatic vessels have a smooth muscle cell (SMC) layer that helps to pump the lymph forward while the luminal valves in these vessels prevent the backflow (Oliver and Detmar

[6]Corresponding author.
E-MAIL rklein@neuro.mpg.de; FAX 49-8985783152.
Article and publication are at http://www.genesdev.org/cgi/doi/10.1101/gad.330105.

2002). Reflecting the functional diversity, the antigenic profile of the blood vascular endothelium varies in different types of vessels and in different organs (Ruoslahti 2004). In contrast to blood vascular endothelium, very little is known of the heterogeneity of the lymphatic endothelium in different vessel types.

Because of their common origin, the molecular mechanisms regulating the development of blood and lymphatic vasculatures are partially shared. Formation of the early blood vascular plexus is highly dependent on vascular endothelial growth factor (VEGF) signaling through its receptors VEGFR-1 and VEGFR-2 (for review, see Rossant and Howard 2002). In contrast, another member of the VEGF family, VEGF-C, has a critical role in the regulation of the growth of lymphatic vessels via the LEC receptor, VEGFR-3 (Jeltsch et al. 1997; Veikkola et al. 2001; Karkkainen et al. 2004). After the initial vascular formation further remodeling of both blood and lymphatic vasculatures seems to require continued VEGF/VEGF-C signaling in co-operation with the regulation of the activity of Tie receptor tyrosine kinases by Angiopoietins (Gale et al. 2002; for review, see Thurston 2003). In addition, the remodeling of the primary blood capillary plexus and the formation of major vessels require signaling mediated by ephrinB2 and its receptors (Wang et al. 1998; Adams et al. 1999; for review, see Adams 2002). However, the expression of different ephrins and Eph receptors in the lymphatic system and their involvement in lymphatic development has not been previously examined.

In the blood vasculature, ephrinB2 is expressed in the arterial endothelial and SMCs, whereas EphB4 is present in the endothelium of veins (Wang et al. 1998; Adams et al. 1999; Shin et al. 2001). The interaction between ephrinB2 and EphB4 may provide the critical repulsion signals required to set arterial–venous boundaries, reminiscent of their repulsive guidance of axonal growth cones. However, ephrinB–Eph interaction can also stimulate endothelial cell sprouting (Adams et al. 2001; Palmer et al. 2002), and therefore the outcome of this interaction may depend on the cellular context and on the involvement of other signaling components, such as growth factor receptors. Molecularly, the ephrinB–Eph system can function bidirectionally: As for most other receptor tyrosine kinases, ligand binding induces "forward" signaling, mainly through phosphotyrosine-mediated pathways. But ephrins can also signal into their host cell—referred to as "reverse" signaling (for review, see Kullander and Klein 2002). The ephrinB cytoplasmic tail can be phosphorylated by Src-family kinases in their tyrosine residues, which provide docking sites for intracellular signaling molecules (Palmer et al. 2002). EphrinBs also have a C-terminal motif for the binding of PDZ-domain containing proteins (Lu et al. 2001; Palmer et al. 2002 and references within). In vivo, certain morphogenetic processes such as segmentation and axon guidance have been shown to require ephrinB cytoplasmic sequences in addition to Eph forward kinase signaling (for review, see Davy and Soriano 2005; Cowan et al. 2004; Dravis et al. 2004). The role of ephrinB2 cytoplasmic sequences in angiogenesis, however, is controversial (see below). In addition, the signaling pathways downstream of ephrin reverse signaling that are required in vivo are not well understood. A recent report suggested that the related ephrinB1 required its PDZ target site for the elevation and fusion of palatal shelves, a complex process that involves cell migration, adhesion, and cell reprogramming (Davy et al. 2004).

In order to get further insights into the mechanisms of ephrinB2 signaling, we have generated two novel knock-in alleles of ephrinB2: *ephrinB2*$^{\Delta V}$ mice expressed ephrinB2 lacking the C-terminal valine within the PDZ interaction site, and *ephrinB2*^{5F} mice expressed ephrinB2 in which five conserved tyrosine residues were replaced by phenylalanine to disrupt phosphotyrosine-dependent signaling events. The analysis of the homozygous *ephrinB2*$^{\Delta V/\Delta V}$ and *ephrinB2*$^{5F/5F}$ mice revealed that these mice survive the requirement of ephrinB2 in embryonic vascular remodeling. However, *ephrinB2*$^{\Delta V/\Delta V}$ mice developed chylothorax and exhibited major lymphatic defects, including hyperplasia, lack of luminal valve formation, and failure in the lymphatic remodeling, which were largely rescued in *ephrinB2*$^{5F/5F}$ mice. The observed lymphatic defects revealed hitherto undescribed remodeling events in skin lymphangiogenesis and establish ephrinB2 as an essential component in post-natal lymphatic development.

Results

Generation of hypomorphic ephrinB2 *alleles*

To investigate novel ephrinB2 isoforms deficient in cytoplasmic interactions, we first generated the corresponding cDNAs and expressed them in heterologous expression systems (HeLa cells and HEK293 cells) (Fig. 1A). To be able to compare relative protein levels and plasma membrane targeting of transfected constructs, we attached yellow fluorescent protein (YFP) to their extreme N terminus, a modification that does not interfere with surface expression or receptor binding (Zimmer et al. 2003). All ephrinB2 isoforms including wild-type ephrinB2 (ephrinB2^{WT}), ephrinB2 lacking the C-terminal valine within the PDZ interaction site (ephrinB2$^{\Delta V}$), and ephrinB2 in which five conserved tyrosine residues were replaced by phenylalanine (ephrinB2^{5F}) were efficiently expressed as judged by Western blot analysis against YFP (data not shown). Plasma membrane targeting was confirmed by the ability of cells transfected with these constructs to bind soluble EphB4-AP fusion protein (Fig. 1B). We also used the surface-binding assay to address the controversy (Davy and Soriano 2005) about plasma membrane localization of two independently generated cytoplasmic deletion (ΔC) mutants. EphrinB2$^{\Delta C}$ protein previously studied in our laboratory (Adams et al. 2001) carries 14 amino acids corresponding to the ephrinB2 cytoplasmic tail followed by the hemagglutinin (HA) epitope tag (here referred to as ephrinB2$^{\Delta C\text{-}HA}$) (Fig. 1A). Transfected cells expressing ephrinB2$^{\Delta C\text{-}HA}$ bound EphB4-AP as well as the cells expressing wild-type ephrinB2, indicating efficient plasma membrane localiza-

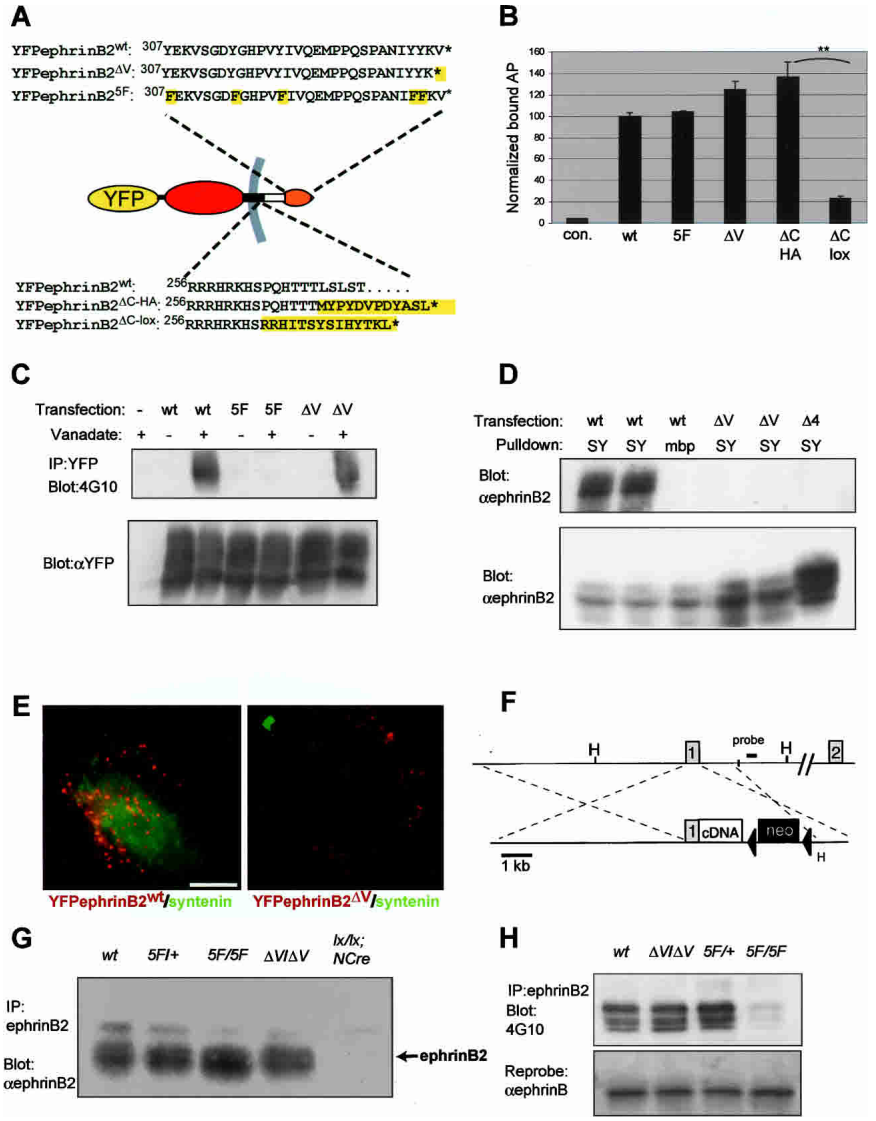

Figure 1. Generation and validation of novel ephrinB2 cDNA knock-in mutants. (*A*) Schematic representation of YFP-ephrinB2 mutants with the relevant amino acid sequence alterations in their cytoplasmic tails. (*Top*) EphrinB2$^{\Delta V}$ and ephrinB2^{5F} compared with wild-type ephrinB2. (*Bottom*) Previously reported alleles of *ephrinB2* including a substitution of HA-tag for the cytoplasmic domain (ephrinB2$^{\Delta C\text{-}HA}$; Adams et al. 1999) and a substitution of the ORF encoded by a loxP site for the cytoplasmic domain (ephrinB2$^{\Delta C\text{-}lox}$; Dravis et al. 2004). (*B*) Quantitative analysis of surface ephrinB2 in HeLa cells transiently transfected with GFP (control, *left*-most lane) or ephrinB2 wild-type or mutant constructs, as assayed by binding of EphB4–alkaline phosphatase fusion protein. Results of a representative experiment are presented as the average of bound alkaline phosphatase activity divided by total expressed protein and normalized to values for the wild-type construct (see Materials and Methods). Transfection of cells with wild-type (WT), 5F, ΔV, or ΔC-HA ephrinB2 expression plasmids result in robust binding of EphB4-AP, whereas ΔC-lox transfected cells exhibit little surface-binding activity, consistent with the protein product being trapped in the trans-Golgi network (Cowan et al. 2004). ** indicates $p < 0.01$ for triplicate measurements, Student's two-tailed *t*-test. (*C*) EphrinB2 tyrosine phosphorylation after vanadate treatment. Hela cells transiently transfected with wild-type (WT), tyrosine mutant (5F), or PDZ site-deficient (ΔV) ephrinB2 constructs were stimulated with vanadate and lysed. Immunoprecipitated ephrinB2 was analyzed by anti-phosphotyrosine (4G10) and total ephrinB2 by anti-YFP Western blot. (*D*) Interaction of ephrinB2 with PDZ proteins. HeLa cells transiently transfected with wild-type (WT) or PDZ-binding site-deficient (ΔV, Δ4) ephrinB2 constructs were lysed and the lysates subjected to pull-down using bacterially produced syntenin1 fused to maltose-binding protein (SY) or unfused maltose-binding protein (MBP). (*Top*) The resultant pull-downs were analyzed by anti-ephrinB2 Western blot. (*Bottom*) Pull-down input was analyzed by Western blot against ephrinB2 on total lysates. (*E*) Colocalization of PDZ domain containing protein, syntenin, with ephrinB2. Hela cells transiently transfected with wild-type (WT) or PDZ-binding site-deficient (ΔV) YFP-ephrinB2 constructs. Cells were stimulated for 30 min with clustered EphB4-Fc receptor bodies to induce ephrinB2 clustering (Zimmer et al. 2003). A mutant GFP-tagged syntenin, lacking PIP2-binding activity, colocalized robustly with patches of ephrinB2^{WT} (*left* panel) but not with ephrinB2$^{\Delta V}$ (*right* panel). Bar, 10 µm. (*F*) Targeting strategy for the generation of mutant mice expressing *ephrinB2^{5F}* or *ephrinB2$^{\Delta V}$*. Exon 1 (gray box) contains the 5′ end of the ORF. The depicted cDNA knock-in strategy was described previously (Adams et al. 2001; see also Materials and Methods). The loxP-flanked (black triangles) neomycin selection marker (black box) was subsequently removed by intercrossing with a mouse line transgenic for Cre recombinase. HindIII restriction sites ("H") and the probe used for Southern hybridization are indicated. (*G*) EphrinB2 expression levels in adult brain lysates. EphrinB2 was immunoprecipitated from total adult brain lysates of wild-type and heterozygous (5F/+), homozygous (5F/5F and ΔV/ΔV) knock-in mice, or ephrinB2lx/lx;Nestin-Cre mutants (lx/lx;NCre) (Grunwald et al. 2004). The resulting precipitates were analyzed by anti-ephrinB2 Western blot. Mutant ephrinB2 is translated to approximately native levels. (*H*) EphrinB2 tyrosine phosphorylation in E12.5 embryos. EphrinB2 was immunoprecipitated as in *G* from E12.5 wild-type and homozygous mutant animals and the precipitates analyzed for phosphotyrosine content by anti-phosphotyrosine (4G10) Western blot. Total ephrinB2 was analyzed by anti-ephrinB2 Western blot.

tion. In contrast, another deletion mutant described by Cowan et al. (2004) carries only eight amino acids corresponding to the ephrinB2 cytoplasmic tail followed by sequences encoded by the in-frame loxP sequence (here referred to as ephrinB2$^{\Delta C\text{-}lox}$). Although this protein was efficiently expressed, the transfected cells showed strongly reduced EphB4-AP binding, indicating poor trafficking to the plasma membrane (Fig. 1B). The average

value of normalized EphB4-AP binding of ephrinB2$^{\Delta C\text{-}HA}$ was 7.2× greater than that determined for ephrinB2$^{\Delta C\text{-}lox}$ ($4.5 \pm 2.7 \times 10^{-9}$ vs. $0.62 \pm 0.2 \times 10^{-9}$ OD/minute/light abundance unit, $n = 3$ independent experiments). Moreover, YFP fluorescence of cells expressing ephrinB2^{WT} and ephrinB2$^{\Delta C\text{-}HA}$ proteins showed diffuse cytoplasmic and plasma membrane staining, whereas most of the ephrinB2$^{\Delta C\text{-}lox}$ protein aggregated within the cytoplasm, possibly in the trans-Golgi network as suggested previously (Cowan et al. 2004; Dravis et al. 2004; Supplementary Fig. S1). These results indicate that all the cytoplasmic mutant ephrinB2 isoforms, except the ephrinB2$^{\Delta C\text{-}lox}$ protein, are targeted to the cell surface. EphrinB2$^{\Delta C\text{-}HA}$, although possibly deficient in vivo in other behaviors besides reverse signaling (see Discussion), behaves in a qualitatively different manner from the protein null ephrinB2$^{\Delta C\text{-}lox}$ in transfected cells.

To further validate the behavior of the novel ephrinB2 point mutants, we treated transiently transfected HeLa cells with the tyrosine phosphatase inhibitor vanadate to allow maximum tyrosine kinase activity (Fig. 1C). While immunoprecipitated tagged wild-type and ephrinB2$^{\Delta V}$ proteins showed phosphotyrosine signal following this potent stimulus, ephrinB2^{5F} was not phosphorylated, confirming that cytoplasmic tyrosine phosphorylation sites are missing in the ephrinB2^{5F} protein. To evaluate the alteration of PDZ binding in the ephrinB2$^{\Delta V}$ mutant protein, we transfected tagged ephrinB2 constructs into HeLa cells and subjected them to pull-down using a known ephrinB2 interactor, syntenin-1 fused to MalBP (Koroll et al. 2001). The MalBP–syntenin-1 construct, but not MalBP alone, efficiently pulled down wild-type ephrinB2. EphrinB2$^{\Delta V}$ and an ephrinB2 construct lacking the last four residues, and therefore the whole PDZ-binding domain (ephrinB2$^{\Delta 4}$), were not detectably pulled down by this construct, indicating that the PDZ-binding site was destroyed (Fig. 1D). Finally, we examined the ability of syntenin to colocalize with ephrinB2 in transfected cells. When ephrinB2 clustering was induced by stimulating the cells with EphB4-Fc, syntenin frequently localized with clusters of ephrinB2^{WT}, but it did not colocalize with ephrinB2$^{\Delta V}$ clusters (Fig. 1E).

Having validated the behavior of the cytoplasmic ephrinB2 mutants in transfected cells, we generated knock-in mutant mice by inserting the mouse cDNAs (without the N-terminal YFP tag) into the endogenous mouse *ephrinB2* locus by homologous recombination in embryonic stem cells (Fig. 1F). Germline mutant mice were generated using standard protocols and the neomycin cassette was subsequently removed in the progeny by Cre-mediated excision. The severity of the phenotype of *ephrinB2*$^{\Delta V/\Delta V}$ mice was dependent on the presence of neomycin cassette and on the genetic background (see Materials and Methods). For further analyses, all *ephrinB2* alleles were kept on a genetic background enriched for C57/Bl6 (at least three times outcrossed). We validated correct expression of ephrinB2 protein by comparing the expression levels in adult brain (in CD1 genetic background where all the mutants showed normal viability). Animals homozygous for either *ephrinB2*^{5F} or *ephrinB2*$^{\Delta V}$ knock-in alleles showed approximately wild-type levels of ephrinB2 expression (Fig. 1G). To assess tyrosine phosphorylation in vivo, we immunoprecipitated ephrinB2 from E12.5 embryos and probed using 4G10 anti-phosphotyrosine antibodies. *ephrinB2*$^{5F/5F}$ mutants showed a strongly reduced phosphotyrosine signal relative to wild-type embryos (Fig. 1H). Residual signal may represent tyrosine phosphorylated coprecipitated ephrinB1 or ephrinB3.

EphrinB2 PDZ interaction but not tyrosine phosphorylation is required for normal development of lymphatic vasculature

Homozygous *ephrinB2*$^{\Delta V/\Delta V}$ and *ephrinB2*$^{5F/5F}$, as well as control *ephrinB2*$^{WT/WT}$ mice, were born in expected Mendelian ratio, indicating that these mice survived the requirement of ephrinB2 in embryonic blood vascular remodeling. While *ephrinB2*$^{5F/5F}$ and *ephrinB2*$^{WT/WT}$ mutant mice survive to adulthood, *ephrinB2*$^{\Delta V/\Delta V}$ mutants in C57Bl/6 background died during the first 3 wk after birth. Cadavers were frequently found with effusion of chyle from the thoracic duct into the pleural space, a condition called chylothorax (Fig. 2A). The death of the mice is likely due to synergized effect of the defects in the lymphatic vasculature with the failure in blood vascular remodeling of the lung (G.A. Wilkinson, T. Mäkinen, and R. Klein, unpubl.). Before the appearance of chylothorax, chylous fluid was often detected in lymphatic vessels in the thoracic area, such as in the lymphatics on the heart pericardium and on the rib cage (data not shown). Normally, chyle is present only in the mesenteric lymphatic vessels, cisterna chyli, and thoracic duct, and therefore the presence of chylous fluid in any other body cavity or tissue implies leakage or backflow of lymph from the central lymphatic channels. In addition, several mutant mice had red blood cells in the lymphatic vessels (data not shown), suggesting a possible failure in the separation of the blood and lymphatic systems. The phenotype suggested an important role for ephrinB2 PDZ interaction in the normal development of the lymphatic vasculature.

EphrinB2 is expressed in the endothelial cells of collecting lymphatic vessels

To begin addressing the role of ephrinB2 in lymphatic vessel development, we first investigated ephrinB2 expression using a lacZ reporter mouse (Wang et al. 1998). As previously reported (Gale et al. 2001; Shin et al. 2001), ephrinB2 expression was detected in the arterial endothelium and in the SMCs surrounding arteries and some veins, while the venous endothelium was negative for ephrinB2 expression (Fig. 2B–E, Supplementary Fig. 2A–C). Rather unexpectedly, we found strong expression of ephrinB2 in the endothelial cells of collecting lymphatic vessels, including the lymphatic vessels surrounding the ischiatic vein (Fig. 2B), in the subcutaneous fat (Fig. 2C), in the mesentery (Fig. 2D), and the thoracic duct (Fig. 2E; see also Supplementary Fig. 2A–C). Collecting lymphatic

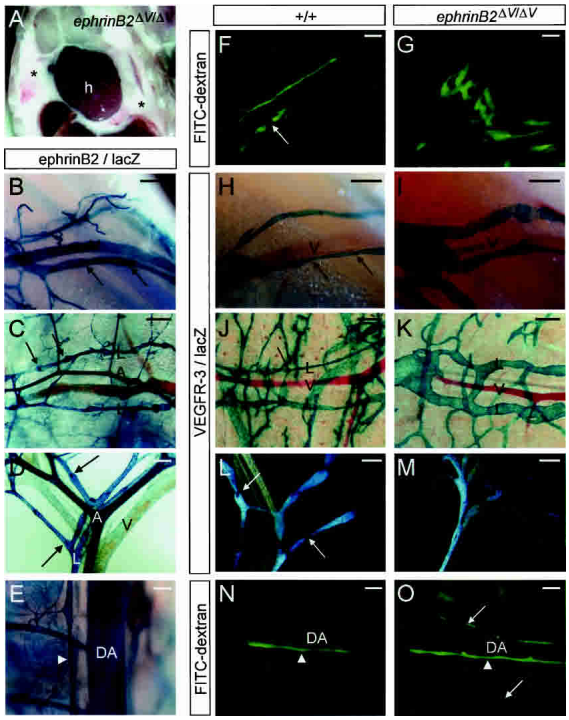

Figure 2. Collecting lymphatic vessels are hyperplastic and unvalved in *ephrinB2*$^{\Delta V/\Delta V}$ mice. (*A*) Chylothorax in an *ephrinB2*$^{\Delta V/\Delta V}$ mutant mouse. Gross dissection of the chest cavity of a P6 *ephrinB2*$^{\Delta V/\Delta V}$ mutant cadaver showing chest cavity filled with chyle (*). (h) Heart. (*B–E*) X-Gal staining in heterozygous *ephrinB2*$^{LZ/+}$ reporter mice. In addition to strong expression in the arterial endothelium and SMCs, *ephrinB2* promoter activity is detected in the endothelium of collecting lymphatic vessels surrounding the ischiatic vein (*B*), in the skin (*C*), mesentery (*D*), and thoracic duct (white arrowhead, *E*). (*B–D*) While venous endothelium (V) is negative for ephrinB2 expression, the SMCs surrounding larger veins are positive (see also Supplementary Fig. S2). Luminal valves are indicated with black arrows. (L) Lymphatic vessel; (A) artery; (V) vein; (DA) dorsal aorta. (*F–O*) Fluorescent lymphoscintiography of the collecting lymphatic vessels surrounding the ischiatic vein (*F,G*) and of the thoracic duct (*N,O*) after high-molecular-weight FITC-dextran injection into the hindlimb footpad of wild-type (*F,N*) and *ephrinB2*$^{\Delta V/\Delta V}$ mutant (*G,O*) mice. X-Gal staining of lymphatic vessels in *VEGFR3*$^{LZ/+}$ mice of ischiatic vein region (*H,I*), collecting lymphatic vessels of the skin (*J,K*), and mesenteric lymphatic vessels (*L,M*) of the indicated genotypes (*top*). The collecting lymphatic vessels are hyperplastic in the mutant mice (*G,I,K*) and lack the luminal valves present in wild-type mice (arrows in panels *F,H,J,L*). The thoracic duct is indicated by white arrowheads in panels *N* and *O*; the leakage and reflux of FITC dextran dye into the side branches in *ephrinB2*$^{\Delta V/\Delta V}$ mutant mouse is indicated by white arrows in *O*. Bars: *B–D,F–M*, 200 µm; *E,N,O*, 500 µm. Ages of the mice: *B,F–I,N,O*, P10; *D,E,L,M*, P5; *C,J,K*, P1.

vessels were identified by the presence of characteristic valves (arrows in Fig. 2B–D) and by their chylous fluid content, as well as by the expression of the lymphatic endothelial cell-specific marker, VEGFR-3 (Dumont et al. 1998; Supplementary Fig. 2B). Moreover, we found that cultures of LECs expressed ephrinB2 and its cognate receptor EphB4 (Supplementary Fig. 2D). We also analyzed the expression of EphB4 using a lacZ reporter mouse (Gerety et al. 1999) and found that EphB4 was expressed in vivo in the endothelium of lymphatic vessels, including the thoracic duct and the lymphatic vessels in the mesentery and in the skin (Supplementary Fig. S2E–G).

Collecting lymphatic vessels are hyperplastic and unvalved in ephrinB2$^{\Delta V/\Delta V}$ *mice*

Because of the strong expression of ephrinB2 in the collecting lymphatic vessels, we analyzed the morphology and function of these vessels in the *ephrinB2* mutant mice. To directly evaluate lymphatic function, we investigated uptake and transport of large-molecular-weight fluorescent (FITC) dextran, which was injected subcutaneously into the footpads. In wild-type mice, the FITC dextran injected into the hindlimb footpad was rapidly drained into the small-diameter, valved collecting lymphatic vessels surrounding the ischiatic vein (Fig. 2F). However, these collecting vessels were severely hyperplastic in *ephrinB2*$^{\Delta V/\Delta V}$ mutant mice (Fig. 2G). To monitor the anatomy of the lymphatic vessels, we intercrossed the ephrinB2 mutants with mice carrying the lacZ gene in the VEGFR-3 locus (*VEGFR3*^{LZ} allele) (Dumont et al. 1998). The hyperplastic morphology of the collecting lymphatic vessels in the ischiatic vein region (Fig. 2H,I) as well as in the skin (Fig. 2J,K) was confirmed by β-Gal staining of *ephrinB2*$^{\Delta V/\Delta V}$;*VEGFR3*$^{LZ/+}$ mutants. In contrast, the vessels appeared normal in *ephrinB2*$^{5F/5F}$ and *ephrinB2*$^{WT/WT}$ mutant mice carrying the *VEGFR3*^{LZ} allele (data not shown).

In the wild-type mice the collecting lymphatic vessels have luminal valves, which prevent the backflow of the lymph (arrows in Fig. 2F,H,J,L). However, no valves were detected in the *ephrinB2*$^{\Delta V/\Delta V}$ mutant mice (Fig. 2G,I,K,M). Due to the lack of valves, reflux of FITC-dextran dye was observed in the mutants, for example, from the major collecting channel, the thoracic duct, into the side branches (Fig. 2N,O).

In summary, these results suggest defects in the morphology and in the luminal valve formation in collecting lymphatic vessels in *ephrinB2*$^{\Delta V/\Delta V}$ mutant mice. In contrast, the formation of collecting lymphatic vessels appeared normal in *ephrinB2*$^{5F/5F}$ and *ephrinB2*$^{WT/WT}$ mutant mice (Supplementary Fig. 3A–D; data not shown)

EphrinB2 PDZ-binding site is required for the remodeling of the dermal lymphatic vasculature

In order to get further insights into the mechanisms by which the phenotype arose, we used *ephrinB*$^{LZ/+}$ and *VEGFR-3*$^{LZ/+}$ mice to visualize the formation of dermal lymphatic vessels during post-natal development in wild-type and *ephrinB2* mutant mice. In newborn mice, the dermal lymphatic vasculature forms a primitive plexus of large diameter vessels in deeper dermal layers

(Fig. 3A,C). These initial capillaries express ephrinB2 (Fig. 3G) as well as EphB4 (Fig. 3H). The primitive plexus is then further remodeled; post-natal day 2 (P2) skin shows the subtle beginnings of pointed sprouts emerging from the initial capillaries (Fig. 3E,e′). In areas where sprouting is more advanced, the lymphatic vessels have produced secondary and tertiary sprouts that invade upper dermal layers (Fig. 3I). Sprouts extend into upper dermal layers to form a superficial capillary plexus (arrows in Fig. 3I,K,M). After the formation of the two vessel layers, ephrinB2 expression is maintained in the precollector vessels in the deeper dermal layers, whereas the superficial capillary plexus did not show detectable ephrinB2 expression (Fig. 3O). Instead, EphB4 expression is detected both in the capillaries and in the precollecting lymphatic vessels (data not shown; see Fig. 6I–L, below).

We found that the initial lymphatic vascular plexus in the newborn skin formed normally in *ephrinB2*$^{\Delta V/\Delta V}$; *VEGFR3*$^{LZ/+}$ mutant mice (Fig. 3B,D). However, the sprouting of endothelial cells was disturbed (Fig. 3F,f′,J). While the initiation of sprout formation appeared to occur, the cells failed to take the characteristic elongated morphology of a sprouting endothelial cell; rather the mutant plexus depicted few rounded bumps suggesting aborted attempts of sprouting (Fig. 3F,f′). The failure in sprout formation resulted in the reduction or absence of the formation of the superficial capillary network (Fig. 3L,N, Supplementary Fig. S4C,D). In contrast to the mice expressing ephrinB2$^{\Delta V}$, control knock-in mutants expressing either wild-type ephrinB2 or ephrinB2^{5F} displayed a normal lymphatic vessel network (data not shown; Supplementary Fig. S4E–H).

The presence of the *VEGFR3*^{LZ} allele may lead to reduced protein levels of VEGFR-3, which is a major regulator of lymphangiogenesis, and therefore enhance the lymphatic phenotype in the *ephrinB2* mutants. Therefore we also stained skin biopsies from *ephrinB2* mutants wild type for the *VEGFR-3* allele with antibodies against VEGFR-3 and LYVE-1, commonly used markers for lymphatic endothelium (see Materials and Methods). In *ephrinB2*$^{\Delta V/\Delta V}$ mutants lacking the *VEGFR3*^{LZ} allele the lymphatic phenotype was qualitatively similar, yet somewhat milder, than in *ephrinB2*$^{\Delta V/\Delta V}$;*VEGFR3*$^{LZ/+}$ mutants. Precollecting vessels were markedly hyperplastic (data not shown). However, the formation of the superficial capillary plexus occurred to some extent, but the superficial capillaries were also hyperplastic (Supplementary Fig. S4I–L).

EphrinB2 has an important function in the remodeling of the early embryonic blood vasculature (Wang et al. 1998; Adams et al. 1999). Therefore, we also analyzed the dermal blood vessels in the *ephrinB2* mutants to find out if the blood vasculature had the same requirements for ephrinB2 PDZ interactions as the lymphatic vessels. Staining of the ear skin for pan-endothelial cell marker PECAM-1 showed normal hierarchical architecture of blood vessels and capillaries in the *ephrinB2*$^{\Delta V/\Delta V}$ mice when compared with the wild-type mice (Supplementary Fig. S4M,N). In addition, we intercrossed *ephrinB2*$^{\Delta V/\Delta V}$ mutants with the *tie2-lacZ* marker line (Schlaeger et al. 1997) to specifically stain the blood vessels. The general architecture of smaller and larger blood vessels was observed in the controls and *ephrinB2*$^{\Delta V/\Delta V}$;*tie2-lacZ* mutants, although especially in the older mutants the larger

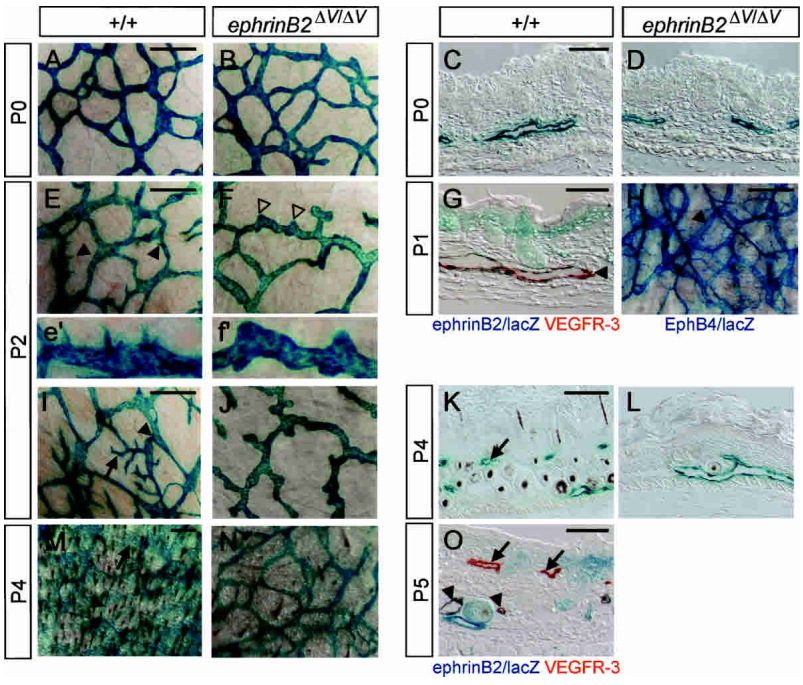

Figure 3. Defective remodeling of the lymphatic capillary plexus in *ephrinB2*$^{\Delta V/\Delta V}$ mutant skin. Whole-mount X-gal staining in the *VEGFR3*$^{LZ/+}$ background of wild-type (+/+; *A*,*E*,*e*′,*I*,*M*) and *ephrinB2*$^{\Delta V/\Delta V}$ (*B*,*F*,*f*′,*J*,*N*) mutant skin (respective sections in panels *C*,*D*,*K*,*L*). Ventral skin biopsies were taken from mice at the indicated ages (P0–P5). Sprouts forming from the primary plexus in wild-type skin are indicated by filled arrowheads in panel *E* (higher magnification in *e*′), secondary and tertiary sprouts by a black arrow in panel *I*. (*K*,*M*,*O*) Sprouts elongate to upper dermal layers and form a superficial lymphatic capillary plexus (arrows). In the mutants, the sprouting is disturbed (open arrowheads in *F*, higher magnification in *f*′), which leads to failure in the formation of the superficial capillary plexus (*J*,*L*,*N*). (*G*,*O*) Combined X-Gal and anti-VEGFR-3 staining in heterozygous *ephrinB2*$^{LZ/+}$ skin at P1 (*G*) and at P5 (*O*). Note double staining of primary lymphatic capillary plexus and smaller diameter precollectors (arrowheads in *G*,*O*, respectively) for ephrinB2 (X-Gal; blue) and VEGFR-3 (IHC; red). (*O*) The post-remodeling superficial plexus is ephrinB2 negative (arrows). (*G*,*O*) In addition to endothelial cells, ephrinB2 is also expressed in hair follicles and upper layers of the dermis. (*H*) X-Gal staining of *EphB4*$^{LZ/+}$ skin at P1 revealed EphB4 expression in primary lymphatic capillaries (arrowhead) in addition to veins. Bars, *left* panels and *H* (whole mounts), 200 µm; *right* panels (sections), 50 µm. (*e*′,*f*′) Higher magnifications from *E* and *F*.

arteries appeared to become slightly contorted, possibly due to the lymphatic defects that may lead to tissue edema (Supplementary Fig. S4O,P). We therefore concluded that expression of ephrinB2 with an intact PDZ-binding site was essential for lymphatic, but not blood vascular remodeling.

Abnormal lymphatic drainage with dermal reflux in ephrinB2$^{\Delta V/\Delta V}$ mice

As shown above, the remodeling of the dermal lymphatic system into a hierarchical network occurs postnatally. Injections of FITC-dextran into the skin of wild-type newborn mice lead to the filling of the whole primitive cutaneous lymphatic capillary network, which is therefore not yet functionally mature (Fig. 4A). Instead, in normal P10 skin, which has undergone the remodeling of the primitive plexus into a vessel network consisting of lymphatic collectors versus capillaries, FITC-dextran was rapidly drained into the small-diameter dermal collecting vessels, which were therefore the only dermal vessels visualized by this method (Fig. 4B). When FITC-dextran was similarly injected into *ephrinB2*$^{\Delta V/\Delta V}$ mutant mice at P10, the dye labeled a vessel network similar to the newborn dermal capillary plexus, as well as hyperplastic collecting vessels, indicating defective fluid transport (Fig. 4D). FITC-dextran injection into *ephrinB2*$^{5F/5F}$ mutant skin revealed a milder phenotype with few dye-labeled branched collecting vessels (Fig. 4E), while control *ephrinB2*$^{WT/WT}$ mice showed a wild-type pattern (Fig. 4C). These data show that the failure in the remodeling of the lymphatic capillary plexus, as well as defective valve formation that allows retrograde flow, leads to abnormal lymphatic drainage and functional failure.

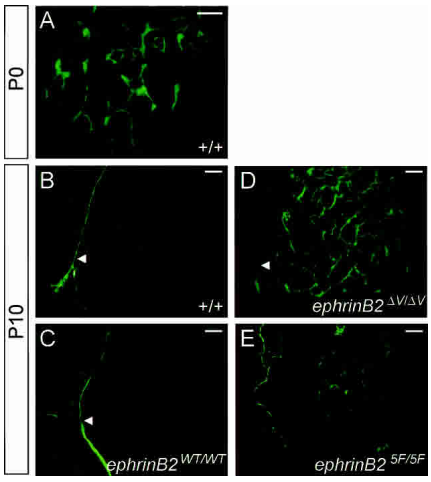

Figure 4. Abnormal lymphatic drainage in *ephrinB2* mutant mice. (*A–E*) Visualization of the dermal lymphatic vessels using fluorescence microscopy after FITC-dextran injection into the forelimb footpad of wild-type mice (+/+) at P0 (*A*) and at P10 (*B*), and of *ephrinB2* knock-in mutants at P10 (*C–E*). (*A*) At P0, the whole primitive dermal lymphatic vessel network is visualized after FITC-dextran injection. At P10, in wild-type (*B*) and knock-in control (*C*) mouse skin, only subcutaneous collecting lymphatic vessels (arrowheads) are visualized, while in *ephrinB2*$^{\Delta V/\Delta V}$ (*D*) and *ephrinB2*$^{5F/5F}$ (*E*) mutant mice a vessel network is observed. Bars, 500 µm.

Failure in the specification of collecting versus capillary lymphatic vessel identity in ephrinB2$^{\Delta V/\Delta V}$ mice

We further analyzed the development of the dermal lymphatic vasculature using ear skin as a model, since due to the thinner dermis it allows a complete whole-mount visualization of the vasculature also in adult mice. As shown by LYVE-1 immunostaining (Fig. 5) and VEGFR3 βgal activity (Supplementary Fig. S5), the remodeling of the lymphatic vasculature in the ear occurred in a similar, although temporally different, manner as in the ventral skin. Sprouts emerged from the initial lymphatic capillary plexus at P4–P5 (Fig. 5E, Supplementary Fig. S5A), and they extended into the upper layer of the dermis, resulting in a two-layered lymphatic vasculature in the wild-type ear at approximately P10: a capillary plexus below the epidermis and a collecting vessel network in the medial part of the ear (Supplementary Fig. S5C). Similar to ventral skin, the early capillary plexus of the ear skin developed normally in the *ephrinB2*$^{\Delta V/\Delta V}$ mutant mice (Fig. 5A,B), but the subsequent development into a hierarchical network failed (Supplementary Fig. S5B,D). In the functional assay, the mutant capillary network was filled with FITC-dextran dye (Supplementary Fig. S5F), while in the normal ear the dye was rapidly drained to the collecting vessels (Supplemental Fig. S5E), reminiscent of the situation in the ventral and back skin (Fig. 4) and suggesting a functional failure.

High-resolution imaging of the ear skin by confocal microscopy revealed that the initiation of the endothelial cell sprouting coincided with the formation of filopodial extensions from the vessels (Fig. 5C), and this process also took place in the *ephrinB2*$^{\Delta V/\Delta V}$ mutant mice (Fig. 5D). The subsequent extension of the sprouting cell (Fig. 5E), which has been recently described during blood vessel development to occur as a guided process, where the tip cell filopodia direct the endothelial cell migration and elongation (Ruhrberg et al. 2002; Gerhardt et al. 2003, 2004), appeared to fail in the mutants, resulting in blunt-ended protrusions (Figs. 5F, 3F,f′,J).

When the two layers of the lymphatic vasculature were formed, the collecting vessels had formed luminal valves and acquired SMC coverage. In parallel with the initiation of the SMC recruitment, the expression of the LYVE-1 marker was down-regulated in the collecting lymphatic vessels (Figs. 5G, 6A–D), especially at the contact sites with the SMCs (data not shown). In the mature vasculature LYVE-1 expression remained high in the lymphatic capillaries while the collecting lymphatic vessels had no or only very weak expression, indicative of a clear distinction of these vessel types not only morphologically but also at the molecular level (Figs. 5G, 6A–D). However, in the *ephrinB2*$^{\Delta V/\Delta V}$ mutant mice, the whole lymphatic capillary network was positive for LYVE-1 staining (Fig. 5H), suggesting a failure in the specification of collecting lymphatic vessel identity.

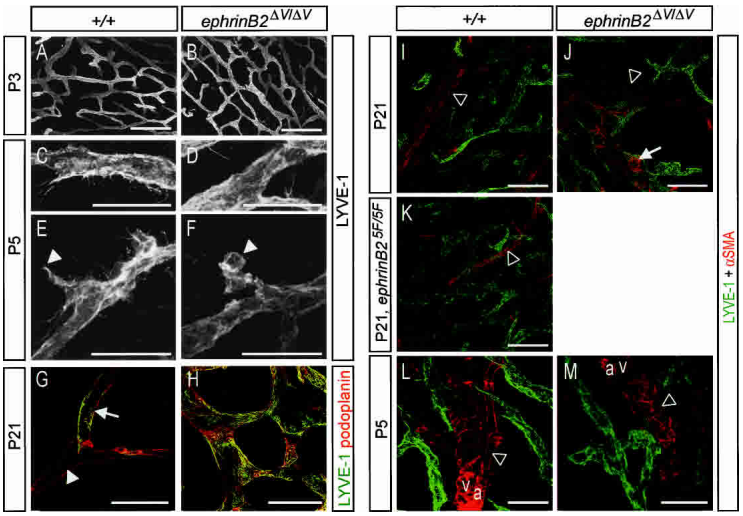

Figure 5. Defective remodeling and abnormal SMC coverage of lymphatic capillaries in *ephrinB2*$^{\Delta V/\Delta V}$ mice. (*A–F*) Immunofluorescence using antibodies against lymphatic-specific marker LYVE-1 of the ear skin at P3 and P5. The formation of the primary lymphatic capillary plexus and the formation of filopodia occurred normally in *ephrinB2*$^{\Delta V/\Delta V}$ mice (*B*,*D*) when compared with wild-type controls (*A*,*C*), but the elongation of the sprouting tip cell (arrowhead in *E*) failed in the mutants, resulting in blunt-ended protrusions (arrowhead in *F*). (*G*,*H*) Double immunofluorescence using antibodies against LYVE-1 (green) and podoplanin (red) of the ear skin at P21. (*G*) Note that in wild-type mice LYVE-1 is expressed in the endothelial cells of lymphatic capillaries (arrow), while podoplanin is expressed both in the capillaries and valved collecting lymphatic vessels (arrowhead). (*H*) In the *ephrinB2*$^{\Delta V/\Delta V}$ mice the whole hyperplastic lymphatic vessel network is LYVE-1 positive. (*I–M*) Double immunofluorescence using antibodies against α-smooth muscle actin (αSMA) for SMCs (red) and against LYVE-1 (green) of the ear skin of the indicated genotypes and ages. (*I–K*) While blood vessels stain positive for αSMA (open arrowheads), the lymphatic capillary network (green) of wild-type and *ephrinB2*$^{5F/5F}$ mice is devoid of αSMA staining both at P5 and P21. (*J*) However, the hyperplastic lymphatic capillaries of *ephrinB2*$^{\Delta V/\Delta V}$ mice at P21 stain positive for αSMA (white arrow pointing to reddish yellow staining). (a) Artery; (v) vein. Bars, *A–F*, 50 µm; *G–M*, 100 µm.

Because some of the lymphatic defects of *ephrinB2*$^{\Delta V/\Delta V}$ mutants could be due to disrupted interactions between lymphatic endothelium and supporting SMCs, which normally cover the collecting but not the capillary lymphatic vessels, we examined lymphatic and blood vessels for their SMC coverage. Costaining of dermal vessels for smooth muscle actin (αSMA) and the lymphatic marker LYVE-1 revealed a lymphatic capillary network uncovered by SMCs in normal control mice both at P21 and P5 (green signal in Fig. 5I,L). The only αSMA-positive structures were blood vessels (open arrowheads in Fig. 5I,L). In contrast, *ephrinB2*$^{\Delta V/\Delta V}$ mutants displayed hyperplastic lymphatic capillaries partially covered with SMCs at P21 (white arrow in Fig. 5J), but not at P5 (Fig. 5M). Importantly, this indicates that the earliest defects in the lymphatic remodeling, which were seen at P5 in *ephrinB2*$^{\Delta V/\Delta V}$ mutant ear skin (Fig. 5F), are detected at a time when the vessels were not yet covered by SMCs (Fig. 5L,M) and desmin-positive pericytes were absent (data not shown). Together with the observation that ephrinB2 is predominantly detected in the lymphatic endothelium, and not in SMCs (Fig. 6E–H), the data suggest a cell-autonomous function of endothelial ephrinB2 in lymphatic remodeling.

In contrast to *ephrinB2*$^{\Delta V/\Delta V}$ mutants, the morphology of the lymphatic capillaries and collecting lymphatic vessels of *ephrinB2*$^{5F/5F}$ mutant mice were normal. In these mice the lymphatic capillaries were uncovered by SMCs (Fig. 5K) and the collecting lymphatic vessels contained normal valves (data not shown).

Differential expression of ephrinB2 and EphB4 in collecting vessels and lymphatic capillaries

Since the lymphatic endothelial cell-specific marker LYVE-1 was predominantly expressed in the lymphatic capillary endothelium while αSMA staining was only seen in the collecting lymphatic vessels in the wild-type skin (Figs. 5G, 6A–D), we used these markers together with a general lymphatic endothelial marker, podoplanin, for the distinction between capillary versus collecting lymphatic vessels. Costaining of ear skin for ephrinB2 (anti-β-Gal), podoplanin, and αSMA confirmed our previous finding that ephrinB2 was specifically detected in lymphatic vessels that contained valves and were covered by SMCs, thus representing collecting lymphatic vessels (Fig. 6E–H). Furthermore, the staining revealed that ephrinB2 was expressed primarily in the lymphatic endothelium but not in the lymphatic SMCs (Fig. 6E–H). Staining of the ear skin for the antibodies against the ephrinB2 receptor, EphB4, together with LYVE-1 and podoplanin antibodies, revealed that EphB4 was expressed in the whole cutaneous lymphatic network, i.e., in LYVE-1-negative valved collecting lymphatic vessels and in LYVE-1-positive lymphatic capillaries (Fig. 6I–L). The expression of EphB4 was not disturbed in *ephrinB2*$^{\Delta V/\Delta V}$ mutants (data not shown).

Abnormal localization of PDZ-domain proteins in lymphatic vessels of ephrinB2$^{\Delta V/\Delta V}$ *mice*

We next attempted to identify a candidate PDZ interactor of ephrinB2 in lymphatic endothelium by screening their expression in wild-type and *ephrinB2*$^{\Delta V/\Delta V}$ mutant tissue. Among the PDZ proteins that have been described to bind ephrinB ligands (Kullander and Klein 2002 and references within; Tanaka et al. 2003), we found that—based on RT–PCR and in situ hybridization—PDZ-RGS3, Dvl2, PICK1/PHIP, Syntenin, GRIP1, and Par3 were expressed in wild-type lymphatic endothelium of the mesenteries (Supplementary Fig. S6; data not shown). Mesenteries were chosen because of the convenient colocalization of lymphatic, arterial, and venous

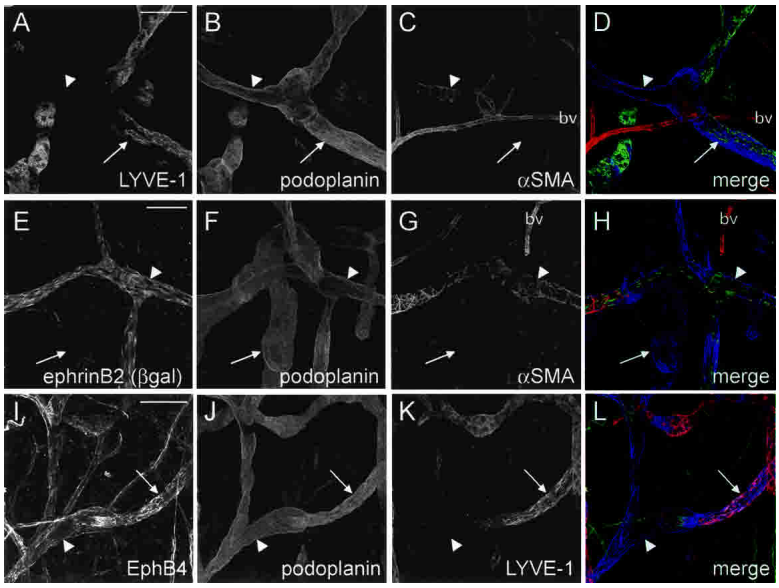

Figure 6. EphrinB2 is expressed predominantly in the endothelial cells of collecting lymphatic vessels, while EphB4 is in both lymphatic capillaries and collecting lymphatic vessels. Triple immunofluorescence for LYVE-1, podoplanin, and αSMA (*A–D*); for ephrinB2 (βgal), podoplanin, and αSMA (*E–H*); and for EphB4, podoplanin, and LYVE-1 (*I–L*) of the ear skin at P21. (*A–D*) High LYVE-1 expression is detected in the lymphatic capillaries (arrow) but not in the αSMA-positive collecting lymphatic vessels (arrowhead). Podoplanin instead stains all lymphatic vessels. αSMA also stains blood vessels (bv). (*E–H*) EphrinB2 is expressed on the endothelium of collecting lymphatic vessels (αSMA-positive, arrowhead), but not on podoplanin-positive, αSMA-negative lymphatic capillaries (arrow). (*I–L*) EphB4 is expressed both on the LYVE-1-positive lymphatic capillaries (arrow) and on the LYVE-1-negative collecting lymphatic vessels (arrowhead). In addition, the veins are positive for EphB4. Bars, 100 µm.

vessels. In contrast, GRIP2 and PTP-BL were not expressed in lymphatic endothelium (Supplementary Fig. S6; data not shown). We then performed immunostainings to ask whether some of these candidate PDZ interactors were expressed in a pattern similar to ephrinB2 and if this pattern was altered in the lymphatic endothelia of *ephrinB2*$^{\Delta V/\Delta V}$ mutant mice.

EphrinB2 protein was expressed mostly in a diffuse pattern in blood vessels (data not shown), whereas the immunoreactivity was conspicuously spotty in lymphatic endothelia, especially near the valves (Fig. 7A–C). This coincided with a spotty localization of candidate PDZ effectors including PICK1, PDZ-RGS3, and Dvl2 in the lymphatic endothelium in wild-type mice (Fig. 7D,F,H). PICK1 signal remained unaltered in the lymphatic vessels of the *ephrinB2*$^{\Delta V/\Delta V}$ mice (Fig. 7E), while PDZ-RGS3 became associated with structures near the cell surface instead of forming clusters (Fig. 7G), a pattern that was observed in immature vessels (data not shown). In addition, Dvl2, which formed clusters enriched at the valve regions, was detected in the *ephrinB2*$^{\Delta V/\Delta V}$ mutants in a diffuse pattern that was hardly above background levels (Fig. 7I). These results suggest that the subcellular distribution of a subset of known PDZ effectors, including RGS3 and Dvl2, depends on the presence of an intact PDZ target site in ephrinB2. RGS3 and Dvl2 are therefore candidate effectors of ephrinB2 reverse signaling during luminal valve formation and remodeling of the lymphatic vasculature. In contrast, PICK1 retains its normal pattern of localization in the mutant mice, perhaps through interaction with alternative binding partners.

Discussion

EphrinB2–EphB4 signaling has been previously shown to have a critical role in the remodeling of the early embryonic blood vasculature partly by defining the boundaries between arteries and veins. The present study extends this concept by implicating ephrinB2 in post-natal lymphangiogenic remodeling. Mice expressing ephrinB2 with a deficient PDZ target site survive the requirement of ephrinB2 in embryonic blood vascular remodeling, but exhibit chylothorax with strong defects in the morphogenesis and function of the lymphatic vasculature. Our findings therefore demonstrate that members of the ephrin family are required for the development of both blood and lymphatic vasculatures, as has been shown for members of the VEGF and Angiopoietin families. These functions are likely due to the disruption of ephrinB2 interaction with downstream PDZ effectors and suggest a requirement for ephrinB2 reverse signaling in lymphatic endothelium. In contrast, phosphotyrosine-mediated signaling was dispensable for ephrinB2 mediated functions in the development of lymphatic, as well as blood vasculature.

Role of ephrinB2 in lymphatic remodeling and maturation

Previous studies have implicated the homeodomain transcription factor Prox1 in the initial specification of lymphatic endothelial cells (Wigle and Oliver 1999; Wigle et al. 2002). Moreover, members of the VEGF family (VEGF-C and VEGF-D) via their cognate receptor VEGFR-3 control the early development of lymphatic vessels by stimulating their sprouting from embryonic veins and by inducing proliferation and survival of lymphatic endothelial cells (Jeltsch et al. 1997; Mäkinen et al. 2001; Veikkola et al. 2001; Karkkainen et al. 2004). Subsequent remodeling of the lymphatic vasculature requires signaling of Angiopoietins and activation of the VEGF-C/VEGFR-3/Neuropilin-2 (Nrp-2) pathway. Lack of Angiopoietin-2 leads to abnormal patterning of lymphatic microvessels and disorganized and hyperplastic lymphatic channels with poor SMC coverage (Gale et al. 2002). In contrast, lack of the VEGF-C/VEGFR-3/Nrp-2

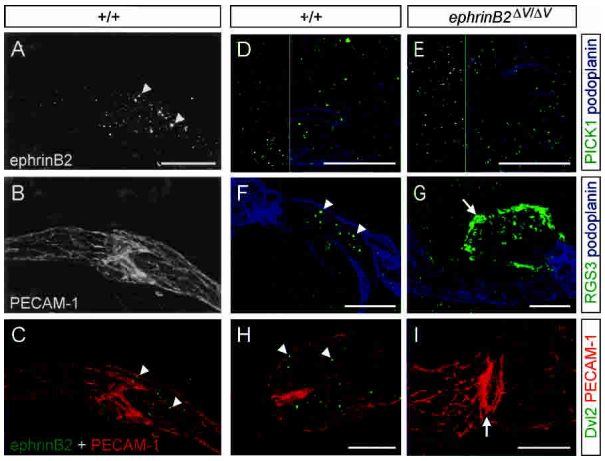

Figure 7. Abnormal localization of ephrinB2 interactors PDZ-RGS3 and Dvl2 in the lymphatic endothelia of *ephrinB2*$^{\Delta V/\Delta V}$ mice. (*A–C*) Double immunofluorescence staining of the ear skin at P21 for ephrinB2 (*A*; green channel in *C*) and for PECAM-1 (*B*; red channel in *C*). (*A*,*C*) Note that ephrinB2 is localized in spots in a region of a lymphatic valve (arrowheads). (*D–I*) Double immunofluorescence staining of the ear skin of wild-type (*D*,*F*,*H*) and *ephrinB2*$^{\Delta V/\Delta V}$ (*E*,*G*,*I*) mice at P21 for PICK1 (green channel in *D*,*E*; *left* part shows PICK1 channel only in b/w) and PDZ-RGS3 (green channel in *F*,*G*) together with podoplanin (blue channel in *D–G*). (*H*,*I*) Double immunofluorescence staining for Dvl2 (green) with PECAM-1 (red). (*F*,*H*) Similar to the localization of ephrinB2, several of the interactors form spots in the lymphatic endothelia in wild-type skin, especially at the valve regions (arrowheads). The localization of PICK1 is not disturbed in *ephrinB2*$^{\Delta V/\Delta V}$ mice (*D*,*E*), while PDZ-RGS3 shows a diffuse staining (arrow in *G*) and Dvl2 is undetectable in the mutant lymphatic vessels, even at the sites where abnormal valve-like structures have formed (arrow in *I*). Bars, 50 μm.

pathway leads to a hypoplastic lymphatic vascular bed (Karkkainen et al. 2001, 2004; Yuan et al. 2002).

While the importance of remodeling has been well established in the formation of a normal, functional blood vasculature (Risau 1997; Carmeliet 2003), little is known about the processes involved in the maturation of the lymphatic system. Here we describe a specific requirement of ephrinB2 for the remodeling of the primary lymphatic capillary plexus and show an important role for this process in building a functional lymphatic vasculature. While the early development of the dermal lymphatic vessels occurred normally in the mutant mice expressing ephrinB2 with a deficient PDZ target site, the maturation of the vasculature into a hierarchical vessel network was disturbed. In wild-type mice, the dermal lymphatic vasculature develops first as a primary capillary plexus, which expresses both ephrinB2 and EphB4, and the subsequent remodeling involves sprouting of new lymphatic capillaries from the initial plexus. The vessels remaining in the deeper dermal layers transform into smaller caliber, valved precollecting lymphatic vessels, which acquire SMC coverage and down-regulate LYVE-1 expression, while maintaining ephrinB2 and EphB4 expression. Instead, the newly formed LYVE-1-positive lymphatic capillaries do not express ephrinB2, while they stay positive for EphB4 expression, suggesting a molecular distinction between collecting versus capillary lymphatic vessels. The interaction between ephrinB2 and EphB4 at the interface of these two vessel types may be required for the establishment of this distinction, similar to the role of ephrinB2–EphB4 interactions at the arterial–venous interface during blood vascular remodeling. In the *ephrinB2*$^{\Delta V/\Delta V}$ mutant mice the specification of the collecting lymphatic vessel identity fails, and therefore the vasculature in the mutant skin resembles morphologically and molecularly a primitive capillary network even in older mice.

As mentioned above, lymphatic capillaries lack pericytes and SMCs, while collecting lymphatic vessels have a sparse SMC coverage. Proper lymphatic endothelial–SMC interaction appears to be critical for the development of functional (collecting) lymphatic vessels and for the formation of luminal valves. Increased SMC coverage in FOXC2-deficient mice leads to abnormal lymphatic patterning and failure in luminal valve formation (Petrova et al. 2004), while impaired recruitment of SMCs in Angiopoietin-2 null mice is associated with disorganization and hyperplasia of lymphatic channels (Gale et al. 2002). We found that in *ephrinB2*$^{\Delta V/\Delta V}$ mice the dermal lymphatic capillaries were sparsely covered by SMCs, raising the question of whether SMCs are responsible for the abnormal lymphatic development in the mutants. However, our data suggest a cell-autonomous function of ephrinB2 in the lymphatic endothelium rather than in adjacent pericytes or SMCs. First, we observed the earliest defects in the lymphatic remodeling in *ephrinB2*$^{\Delta V/\Delta V}$ mutant ear skin at a time when coverage with lymphatic SMCs had not yet begun and desmin-positive pericytes were absent from the dermal lymphatic plexus. Second, ephrinB2 was found to be expressed predominantly in the lymphatic endothelium, not in SMCs. Therefore, the abnormal smooth muscle coverage may result from the misbehavior of the lymphatic endothelium. However, whether or not ephrinB2 has a function in lymphatic SMCs or whether it has additional non-cell-autonomous effects on lymphatic development would have to await the conditional inactivation of ephrinB2 in lymphatic endothelium.

In addition to the remodeling defects, we also found that the development of deeper lymphatic channels was defective in *ephrinB2*$^{\Delta V/\Delta V}$ mutant mice. The collecting vessels were often hyperplastic and lacked the luminal valves. These deficiencies are likely to cause the functional failure and contribute to the development of chylothorax in the homozygous mutant mice. The molecular mechanisms and cellular events required for the formation of luminal valves are unclear. A recent study showed a requirement of a transcription factor FOXC2 for the morphogenesis of lymphatic valves, possibly by maintaining these regions free of SMCs (Petrova et al. 2004). FOXC2 appears to function in lymphatic endothelia by regulating the expression of genes that are involved in maintaining a proper interaction of endothelial cells with SMCs (Petrova et al. 2004). As a transmembrane molecule, ephrinB2 may instead have a direct

function, perhaps in guiding endothelial cell migration and elongation, during valve morphogenesis. The collecting lymphatic vessels in *ephrinB2*$^{\Delta V/\Delta V}$ mice occasionally contained valve-like structures, but in these abnormal structures the endothelial cells seemed to fail to take a proper morphology.

However, not all lymphatic vessels in *ephrinB2*$^{\Delta V/\Delta V}$ mutant mice were affected. For example, the central lymphatic channels of small intestinal villi, the so-called lacteals, and the lymphatic capillaries on the intestinal wall, as well as the lymphatic vessels in the diaphragm, appeared normal in the *ephrinB2*$^{\Delta V/\Delta V}$ mutant mice (Supplementary Fig. S7). In agreement with this, we do not detect accumulation of chylous ascites in the intraperitoneal cavity as has been described in other mouse models in which the intestinal lymphatic vessels were abnormal (Karkkainen et al. 2001; Gale et al. 2002).

Mechanisms of ephrinB2 functions in the development of blood and lymphatic vasculatures

Our demonstration of lymphatic patterning defects in *ephrinB2*$^{\Delta V/\Delta V}$ mutants, together with midline fusion defects in a recently published ephrinB1 PDZ site mutant (Davy et al. 2004), probably represent the best in vivo evidence for the requirement of ephrinB reverse signaling. Previous work from our laboratory (Adams et al. 2001) and others (Cowan et al. 2004; Dravis et al. 2004) using ephrinB2 mutants lacking the entire cytoplasmic region may have some technical limitations and cause a complex readout. Complete C-terminal truncation not only terminates reverse signaling, but also affects protein trafficking and trans-endocytosis of the Eph receptor, thereby affecting Eph forward signaling in neighboring cells (Zimmer et al. 2003). For example, C-terminal truncated ephrinB2 generated by loxP-mediated recombination is not inserted into the plasma membrane and effectively represents a protein null (Cowan et al. 2004; Fig. 1; Supplementary Fig. 1; this report). In contrast, C-terminal truncated ephrinB2 carrying an HA epitope tag is inserted into the plasma membrane as shown by EphB4-AP binding (Adams et al. 2001; Fig. 1; this report) and functions sufficiently in at least some in vivo context (e.g., neural crest migration), but may be acting as a hypomorphic allele in endothelial cells. An ephrinB2–βgal fusion protein, which lacks endogenous cytoplasmic ephrinB2 sequences, rescued the embryonic vascular defects associated with the loss of ephrinB2 by inference, suggesting that EphB forward signaling is sufficient for this process (Cowan et al. 2004). However, the ephrinB2–βgal fusion protein showed elevated expression and behaved genetically dominant with respect to cloacal septation in vivo. Because of the nature of the fusion with tetrameric β-galactosidase, the ephrinB2–βgal fusion protein may also be in a preclustered state that allows more efficient activation of forward signaling. We speculate that elevated surface expression and preclustering of ephrinB2–βgal protein leads to altered (enhanced) EphB forward signaling in the endothelium. This may contribute to the rescue of vascular remodeling.

The recent work on ephrinB1 (Davy et al. 2004) and our findings on ephrinB2 suggest that interactions with PDZ effector proteins are critical for ephrinB reverse signaling in vivo. Among the PDZ proteins that have been described to bind ephrinB ligands, we found that PICK1, PDZ-RGS3, and Dvl2 were expressed in lymphatic endothelium in a spotty pattern resembling the localization of ephrinB2. Moreover, PDZ-RGS3 and Dvl2 localization patterns were altered in *ephrinB2*$^{\Delta V/\Delta V}$ mutant endothelium, consistent with a direct interaction in lymphatic endothelium and with a function as an ephrinB2 effector in this tissue. PDZ-RGS3 has previously been shown to be essential for ephrinB-mediated neuronal cell migration in vitro (Lu et al. 2001); however, its role in lymphangiogenesis has not been explored. Xenopus Dvl has been proposed to mediate ephrinB reverse signaling related to animal cap cell repulsion (Tanaka et al. 2003). Although all Dvl proteins contain a PDZ-binding site, the regions of Dvl and ephrinB that are required for direct interaction have not been fully characterized. Dvl2 knockout mice were reported to suffer from defects in cardiac morphogenesis, somite segmentation, and neural tube closure. However, they die before the development of lymphatic vessels starts (Hamblet et al. 2002). Whether or not loss of Dvl2 leads to similar lymphatic defects as described for *ephrinB2*$^{\Delta V/\Delta V}$ mutants remains to be addressed. PICK1 is mostly known for its involvement in neurotransmitter receptor trafficking at neuronal synapses (Terashima et al. 2004 and references within). The fact that PICK1 immunoreactivity did not change in ephrinB2$^{\Delta V/\Delta V}$ mutants suggests that it has additional interaction partners in lymphatic endothelial cells that organize its subcellular localization independently from ephrinB2. Although our data from transient transfection experiments suggest that syntenin-1 might also be improperly localized in vivo in *ephrinB2*$^{\Delta V/\Delta V}$ mutant animals, we did not consider this candidate effector further because of its poor affinity for ephrinB2^{5F} (data not shown), probably reflecting sensitivity of syntenin-1 to substitutions at the –2 position of substrate C termini (Grootjans et al. 1997; Koroll et al. 2001). Further functional work will be required to identify PDZ proteins that are essential mediators of ephrinB2 signaling in lymphatic endothelia. With >400 genes encoding PDZ domain proteins in the mouse genome (according to SMART database at EMBL), the identification of these molecules may require high-throughput approaches such as affinity purification or protein arrays (MacBeath and Schreiber 2000; Puig et al. 2001).

The lack of a marked phenotype in *ephrinB2*$^{5F/5F}$ mutants (with the exception of a mild lymphatic phenotype characterized by abnormal drainage in the skin) was surprising due to the fact that regulated tyrosine phosphorylation of the ephrinB1 cytoplasmic tail was viewed as the first strong evidence for ephrinB reverse signaling (Holland et al. 1996; Bruckner et al. 1997). It is possible that phosphotyrosine-dependent signaling is more important downstream of ephrinB1 than ephrinB2, and this will have to be addressed genetically. Alternatively, ephrinB2 reverse signaling in the embryo may be complex and

redundant, and defects may only appear when the ephrinB2 cytoplasmic tail is stripped off all tyrosines and the PDZ site is destroyed. Finally, there are additional functions of ephrinB2 that remain to be investigated and may depend on phosphotyrosine signaling, including pathological vascular remodeling in the adult, and axon guidance and neuronal plasticity in the nervous system.

Materials and methods

Antibodies

We used monoclonal rat anti-mouse VEGFR-3 (Kubo et al. 2000), anti-mouse PECAM-1/CD31 (Pharmingen) and hamster anti-mouse podoplanin (RDI), Cy3-conjugated mouse anti-α-SMC actin (Sigma), polyclonal rabbit anti-mouse LYVE-1 (Karkkainen et al. 2004), anti-β-galactosidase (ICN/Cappel), anti-mouse RGS3 (Lu et al. 2001), anti-mouse Dvl2 (Chemicon), anti-GFP (cross-reactive with YFP from RDI), goat anti-mouse EphrinB2 (R&D Systems) and rabbit-anti mouse ephrinB2 (Nikolova et al. 1998), goat anti-mouse EphB4 (R&D Systems), and anti-mouse Pick1 (Santa Cruz) antibodies. Secondary antibodies (conjugated to Alexa488, Cy3, or Cy5) were purchased from Dianova and Jackson Immunoresearch.

Surface-binding assay

Cytoplasmic mutant cDNAs (amino acid sequence illustrated in Fig. 1A) were cloned into a YFP-HA-ephrinB2 wild-type construct (Zimmer et al. 2003), which is based on pYFP-C1 (Stratagene), via the internal BbsI site at nucleotide 894 of mouse ephrinB2 and HindIII. Constructs were transiently transfected into Hela Cells using the calcium phosphate method. EphB4-AP (Brambilla et al. 1996) was prepared separately. Twenty-four hours following transfection, cells were assayed for surface-bindable ephrinB2 following standard protocols (Flanagan and Cheng 2000), except that endogenous phosphatase activity was inactivated for 20 min at 65°C. Raw binding data were normalized to protein levels in total lysates, using anti-YFP Western blot and digitizing software (Fuji LAS 1000 digital camera for ECL and Aida 2.0 densitometry package). Comparison of surface binding of cytoplasmic mutant cDNAs to wild-type ephrinB2 cDNA was performed in triplicate in four independent transfections with similar results.

Vanadate stimulation

Pervanadate was generated by adding 1.1 µL hydrogen peroxide to 1 mL of 100 mM vanadate stocks and added to cells at a final concentration of 0.1 mM for 10 min. Cells were lysed in Triton lysis buffer (50 mM Tris at pH 7.5, 150 mM NaCl, 0.5% Triton X-100) supplemented with 10 mM NaF, 200 mM sodium pyrophosphate, 1 mM vanadate, and Complete Protease Iinhibitors (Roche). YFP-ephrinB2 variants were immune precipitated using anti-GFP antibody, which also recognizes YFP. Precipitates were subjected to Western blot analysis for anti-phosphotyrosine (clone 4G10; Roche).

Pull-down assay

Hela cells were transiently transfected by the $CaPO_4$ method. Cells were lysed in Triton lysis buffer supplemented with Complete Protease Inhibitors (Roche). Clarified lysates were clustered in solution using preclustered recombinant EphB4-Fc protein (R&D Systems, 2 µg/mL). Recombinant pull-down constructs (either maltose-binding protein–syntenin-1 or maltose-binding protein alone) were preloaded onto amylose beads (NEB) and then clustered lysates subjected to pull-down overnight at 4°C.

Colocalization studies

Surface clustering of transiently transfected ephrinB2 variants in Hela cells was induced by stimulation with preclustered EphB4-Fc (R&D Systems; 2 µg/mL) for 30 min at 37°C. Control transfected cells stimulated with preclustered Fc did not show clustering. Subcellular localization of syntenin-1 was assayed by anti-tag immunofluorescence. To prevent confounding colocalization of syntenin with ephrin via its affinity for the raft lipid PIP(2), we used a GFP-syntenin mutant (Zimmermann et al. 2002), which is deficient in these interactions.

Generation of ephrinB2 cDNA knock-in mutant mice

Mouse cDNAs encoding ephrinB2 C-terminal mutant forms ephrinB2^{5F} and ephrinB2$^{\Delta V}$ (amino acid alterations shown in Fig. 1A) were generated by PCR, inserted into pBK-CMV (Stratagene) via ClaI (5′) and SmaI (3′), and sequenced. The cDNAs were isolated together with the SV40 polyadenylation signal from pBK-CMV using MluI (blunted) and ClaI, subcloned into pBK-CMV in reverse orientation (ClaI/ScaI), and then transferred into pFlox3 containing mouse ephrinB2 genomic DNA and a neomycin resistance cassette flanked by lox sites by use of the ClaI site located in the first exon of *ephrinB2* (at position 85 of GenBank MMU30244) and SalI (see also Adams et al. 1999). The linearized targeting construct was electroporated into embryonic stem (ES) cell clones using standard methods and neomycin resistant clones were initially screened using PCR primers spanning the crossover. Potential homologous recombination was detected in 1.2% of neomycin resistant clones. PCR-positive clones were confirmed using Southern blotting on HindIII-digested genomic DNA probed with a fragment 3′ to the recombined region (indicated in Fig. 1F) as well as a neo probe. The neo cassette was subsequently excised from the genomic locus by crossing to a mouse line ubiquitously expressing Cre (PGK-Cre). The presence of neomycin cassette and the genetic background strongly affected the phenotype of the *ephrinB2*$^{\Delta V/\Delta V}$ mice, while homogyzous *ephrinB2*$^{5F/5F}$ and *ephrinB2*$^{WT/WT}$ mice appeared normal in different genetic backgrounds with or without the neo cassette. In C57B1/6 background in the presence of neo cassette the *ephrinB2*$^{\Delta V/\Delta V}$ mice died by P6 and developed a massive chylothorax with milky effusion (Fig. 2A), while with the neo cassette removed the mice often survived 2–3 wk before developing chylothorax with clear effusion. In CD1 background the *ephrinB2*$^{\Delta V/\Delta V}$ mice survived several months and showed only minor defects in the lymphatic vasculature (data not shown), but eventually several of them also developed chylothorax.

Biochemistry

Embryos or adult brains (from CD1 outcross) were homogenized in a dounce homogenizer using Triton lysis buffer supplemented with Complete Protease Inhibitors (Roche), 1 mM sodium vanadate, 10 mM sodium fluoride, and 50 mM sodium pyrophosphate. Lysates were clarified in a microcentrifuge and subjected to ephrinB2 immune precipitation using standard protocols.

Immunohistochemistry

Tissues were fixed with 4% paraformaldehyde (PFA), dehydrated, and embedded in paraffin. Sections (7 µm) were stained after heat-induced epitope retrieval using a Tyramide Signal

Amplification kit (TSA, NEN Life Sciences) and 3-amino-9-ethylcarbazole or diaminobenzidine as a substrate. For whole-mount immunofluorescence stainings, the tissues were fixed with 4% PFA overnight at 4°C, blocked with 3% milk in phosphate buffered saline (PBS) containing 0.3% Triton X-100 and stained overnight at 4°C with the primary antibodies in the blocking solution. After washes, the tissues were incubated with the secondary antibodies for 2 h at room temperature, followed by washing and mounting. The samples were then analyzed by confocal microscopy.

Visualization of blood and lymphatic vessels

The tissues from *VEGFR3*$^{LZ/+}$ (Dumont et al. 1998), *ephrinB2*$^{LZ/+}$ (Shin et al. 2001), *EphB4*$^{LZ/+}$ (Gerety et al. 1999), and *tie2-lacZ* (Schlaeger et al. 1997) reporter mice were fixed with 2% paraformaldehyde or 0.2% glutaraldehyde and stained by the β-galactosidase substrate X-gal (Sigma). After post-fixation in 4% PFA, the tissues were photographed or further processed for sectioning and immunostaining. For the visualization of functional lymphatic vessels, FITC-dextran (Sigma, 8 mg/mL in PBS) was injected subcutaneously into an anesthetized mouse and the lymphatic vessels were analyzed by fluorescence microscopy.

In situ hybridization

Probes were obtained as follows: ephrinB2 (Adams et al. 1999); GRIP1 and GRIP2 (Bruckner et al. 1999); syntenin (clone no. H3030C02) and Par3 (clone no. H3054A01 from the NIA 15K Clone Set, http://lgsun.grc.nia.nih.gov/cDNA/15k.html); PDZ-RGS3, a fragment corresponding to nucleotides 49–619 of NM_134257 (PDZ domain only) obtained by RT–PCR on mouse embryonic brain RNA; Dvl2, a fragment corresponding to nucleotides 876–1352 of NM_007888, obtained by RT–PCR on mouse embryonic brain RNA; and rat PICK1 (rzpd clone IRAKp961P19175Q2 http://www.rzpd.de). Oligonucleotide sequences used to obtain probes are available on request. Segments of intestine containing mesentery and major artery, vein, and valved lymphatic vessel were subjected to whole-mount in situ hybridization using standard methods.

Acknowledgments

We thank F. Diella and K. Vintersten for help with ES cell work and generation of mice, D. Anderson for providing ephrinB2-lacZ and EphB4-lacZ mice, M. Koroll and P. Zimmermann for plasmids, and A. Acker-Palmer for careful reading of the manuscript. G.W. and T.M. were supported by post-doctoral fellowships from the NIH (F32NS10911; G.W.), and from the European Molecular Biology Organization and the Human Frontier Science Program Organization (T.M.). This work was in part funded by the Max-Planck Society and by grants from the Deutsche Forschungsgemeinschaft to R.K. (Kl948/4-3) and by the Swiss National Science Foundation (31-68104.02; A.Z.).

References

Adams, R.H. 2002. Vascular patterning by Eph receptor tyrosine kinases and ephrins. *Semin. Cell Dev. Biol.* **13:** 55–60.

Adams, R.H., Wilkinson, G.A., Weiss, C., Diella, F., Gale, N.W., Deutsch, U., Risau, W., and Klein, R. 1999. Roles of ephrinB ligands and EphB receptors in cardiovascular development: Demarcation of arterial/venous domains, vascular morphogenesis, and sprouting angiogenesis. *Genes & Dev.* **13:** 295–306.

Adams, R.H., Diella, F., Hennig, S., Helmbacher, F., Deutsch, U., and Klein, R. 2001. The cytoplasmic domain of the ligand ephrinB2 is required for vascular morphogenesis but not cranial neural crest migration. *Cell* **104:** 57–69.

Alitalo, K. and Carmeliet, P. 2002. Molecular mechanisms of lymphangiogenesis in health and disease. *Cancer Cell* **1:** 219–227.

Brambilla, R., Bruckner, K., Orioli, D., Bergemann, A.D., Flanagan, J.G., and Klein, R. 1996. Similarities and differences in the way transmembrane-type ligands interact with the Elk subclass of Eph receptors. *Mol. Cell. Neurosci.* **8:** 199–209.

Bruckner, K., Pasquale, E.B., and Klein, R. 1997. Tyrosine phosphorylation of transmembrane ligands for Eph receptors. *Science* **275:** 1640–1643.

Bruckner, K., Pablo Labrador, J., Scheiffele, P., Herb, A., Seeburg, P.H., and Klein, R. 1999. EphrinB ligands recruit GRIP family PDZ adaptor proteins into raft membrane microdomains. *Neuron* **22:** 511–524.

Carmeliet, P. 2003. Angiogenesis in health and disease. *Nat. Med.* **9:** 653–660.

Cowan, C.A., Yokoyama, N., Saxena, A., Chumley, M.J., Silvany, R.E., Baker, L.A., Srivastava, D., and Henkemeyer, M. 2004. Ephrin-B2 reverse signaling is required for axon pathfinding and cardiac valve formation but not early vascular development. *Dev. Biol.* **271:** 263–271.

Davy, A. and Soriano, P. 2005. Ephrin signaling in vivo: Look both ways. *Dev. Dyn.* **232:** 1–10.

Davy, A., Aubin, J., and Soriano, P. 2004. Ephrin-B1 forward and reverse signaling are required during mouse development. *Genes & Dev.* **18:** 572–583.

Dravis, C., Yokoyama, N., Chumley, M.J., Cowan, C.A., Silvany, R.E., Shay, J., Baker, L.A., and Henkemeyer, M. 2004. Bidirectional signaling mediated by ephrin-B2 and EphB2 controls urorectal development. *Dev. Biol.* **271:** 272–290.

Dumont, D.J., Jussila, L., Taipale, J., Lymboussaki, A., Mustonen, T., Pajusola, K., Breitman, M., and Alitalo, K. 1998. Cardiovascular failure in mouse embryos deficient in VEGF receptor-3. *Science* **282:** 946–949.

Flanagan, J.G. and Cheng, H.J. 2000. Alkaline phosphatase fusion proteins for molecular characterization and cloning of receptors and their ligands. *Methods Enzymol.* **327:**198–210.

Gale, N.W., Baluk, P., Pan, L., Kwan, M., Holash, J., DeChiara, T.M., McDonald, D.M., and Yancopoulos, G.D. 2001. Ephrin-B2 selectively marks arterial vessels and neovascularization sites in the adult, with expression in both endothelial and smooth-muscle cells. *Dev. Biol.* **230:** 151–160.

Gale, N.W., Thurston, G., Hackett, S.F., Renard, R., Wang, Q., McClain, J., Martin, C., Witte, C., Witte, M.H., Jackson, D., et al. 2002. Angiopoietin-2 is required for postnatal angiogenesis and lymphatic patterning, and only the latter role is rescued by Angiopoietin-1. *Dev. Cell* **3:** 411–423.

Gerety, S.S., Wang, H.U., Chen, Z.F., and Anderson, D.J. 1999. Symmetrical mutant phenotypes of the receptor EphB4 and its specific transmembrane ligand ephrin-B2 in cardiovascular development. *Mol. Cell* **4:** 403–414.

Gerhardt, H., Golding, M., Fruttiger, M., Ruhrberg, C., Lundkvist, A., Abramsson, A., Jeltsch, M., Mitchell, C., Alitalo, K., Shima, D., et al. 2003. VEGF guides angiogenic sprouting utilizing endothelial tip cell filopodia. *J. Cell Biol.* **161:**1163–1177.

Gerhardt, H., Ruhrberg, C., Abramsson, A., Fujisawa, H., Shima, D., and Betsholtz, C. 2004. Neuropilin-1 is required for endothelial tip cell guidance in the developing central nervous system. *Dev. Dyn.* **231:** 503–509.

Grootjans, J.J., Zimmermann, P., Reekmans, G., Smets, A., Degeest, G., Durr, J., and David, G. 1997. Syntenin, a PDZ protein that binds syndecan cytoplasmic domains. *Proc. Natl. Acad. Sci.* **94:** 13683–13688.

Grunwald, I.C., Korte, M., Adelmann, G., Plueck, A., Kullander,

K., Adams, R.H., Frotscher, M., Bonhoeffer, T., and Klein, R. 2004. Hippocampal plasticity requires postsynaptic ephrinBs. *Nat. Neurosci.* **7:** 33–40.

Hamblet, N.S., Lijam, N., Ruiz-Lozano, P., Wang, J., Yang, Y., Luo, Z., Mei, L., Chien, K.R., Sussman, D.J., and Wynshaw-Boris, A. 2002. Dishevelled 2 is essential for cardiac outflow tract development, somite segmentation and neural tube closure. *Development* **129:** 5827–5838.

Holland, S.J., Gale, N.W., Mbamalu, G., Yancopoulos, G.D., Henkemeyer, M., and Pawson, T. 1996. Bidirectional signalling through the EPH-family receptor Nuk and its transmembrane ligands. *Nature* **383:** 722–725.

Jeltsch, M., Kaipainen, A., Joukov, V., Meng, X., Lakso, M., Rauvala, H., Swartz, M., Fukumura, D., Jain, R.K., and Alitalo, K. 1997. Hyperplasia of lymphatic vessels in VEGF-C transgenic mice. *Science* **276:** 1423–1425.

Karkkainen, M.J., Saaristo, A., Jussila, L., Karila, K.A., Lawrence, E.C., Pajusola, K., Bueler, H., Eichmann, A., Kauppinen, R., Kettunen, M.I., et al. 2001. A model for gene therapy of human hereditary lymphedema. *Proc. Natl. Acad. Sci.* **98:** 12677–12682.

Karkkainen, M.J., Haiko, P., Sainio, K., Partanen, J., Taipale, J., Petrova, T.V., Jeltsch, M., Jackson, D.G., Talikka, M., Rauvala, H., et al. 2004. Vascular endothelial growth factor C is required for sprouting of the first lymphatic vessels from embryonic veins. *Nat. Immunol.* **5:** 74–80.

Koroll, M., Rathjen, F.G., and Volkmer, H. 2001. The neural cell recognition molecule neurofascin interacts with syntenin-1 but not with syntenin-2, both of which reveal self-associating activity. *J. Biol. Chem.* **276:** 10646–10654.

Kubo, H., Fujiwara, T., Jussila, L., Hashi, H., Ogawa, M., Shimizu, K., Awane, M., Sakai, Y., Takabayashi, A., Alitalo, K., et al. 2000. Involvement of vascular endothelial growth factor receptor-3 in maintenance of integrity of endothelial cell lining during tumor angiogenesis. *Blood* **96:** 546–553.

Kullander, K. and Klein, R. 2002. Mechanisms and functions of Eph and ephrin signalling. *Nat. Rev. Mol. Cell Biol.* **3:** 475–486.

Lu, Q., Sun, E.E., Klein, R.S., and Flanagan, J.G. 2001. Ephrin-B reverse signaling is mediated by a novel PDZ-RGS protein and selectively inhibits G protein-coupled chemoattraction. *Cell* **105:** 69–79.

MacBeath, G. and Schreiber, S.L. 2000. Printing proteins as microarrays for high-throughput function determination. *Science* **289:** 1760–1763.

Mäkinen, T., Veikkola, T., Mustjoki, S., Karpanen, T., Catimel, B., Nice, E.C., Wise, L., Mercer, A., Kowalski, H., Kerjaschki, D., et al. 2001. Isolated lymphatic endothelial cells transduce growth, survival and migratory signals via the VEGF-C/D receptor VEGFR-3. *EMBO J.* **20:** 4762–4773.

Nikolova, Z., Djonov, V., Zuercher, G., Andres, A.C., and Ziemiecki, A. 1998. Cell-type specific and estrogen dependent expression of the receptor tyrosine kinase EphB4 and its ligand ephrin-B2 during mammary gland morphogenesis. *J. Cell Sci.* **111:** 2741–2751.

Oliver, G. 2004. Lymphatic vasculature development. *Nat. Rev. Immunol.* **4:** 35–45.

Oliver, G. and Detmar, M. 2002. The rediscovery of the lymphatic system: Old and new insights into the development and biological function of the lymphatic vasculature. *Genes & Dev.* **16:** 773–783.

Palmer, A., Zimmer, M., Erdmann, K.S., Eulenburg, V., Porthin, A., Heumann, R., Deutsch, U., and Klein, R. 2002. EphrinB phosphorylation and reverse signaling: Regulation by Src kinases and PTP-BL phosphatase. *Mol. Cell* **9:** 725–737.

Petrova, T.V., Karpanen, T., Norrmen, C., Mellor, R., Tamakoshi, T., Finegold, D., Ferrell, R., Kerjaschki, D., Mortimer, P., Yla-Herttuala, S., et al. 2004. Defective valves and abnormal mural cell recruitment underlie lymphatic vascular failure in lymphedema distichiasis. *Nat. Med.* **10:** 974–981.

Puig, O., Caspary, F., Rigaut, G., Rutz, B., Bouveret, E., Bragado-Nilsson, E., Wilm, M., and Seraphin, B. 2001. The tandem affinity purification (TAP) method: A general procedure of protein complex purification. *Methods* **24:** 218–229.

Risau, W. 1997. Mechanisms of angiogenesis. *Nature* **386:** 671–674.

Rossant, J. and Howard, L. 2002. Signaling pathways in vascular development. *Annu. Rev. Cell Dev. Biol.* **18:** 541–573.

Ruhrberg, C., Gerhardt, H., Golding, M., Watson, R., Ioannidou, S., Fujisawa, H., Betsholtz, C., and Shima, D.T. 2002. Spatially restricted patterning cues provided by heparin-binding VEGF-A control blood vessel branching morphogenesis. *Genes & Dev.* **16:** 2684–2698.

Ruoslahti, E. 2004. Vascular zip codes in angiogenesis and metastasis. *Biochem. Soc. Trans.* **32:** 397–402.

Schlaeger, T.M., Bartunkova, S., Lawitts, J.A., Teichmann, G., Risau, W., Deutsch, U., and Sato, T.N. 1997. Uniform vascular-endothelial-cell-specific gene expression in both embryonic and adult transgenic mice. *Proc. Natl. Acad. Sci.* **94:** 3058–3063.

Shin, D., Garcia-Cardena, G., Hayashi, S., Gerety, S., Asahara, T., Stavrakis, G., Isner, J., Folkman, J., Gimbrone Jr., M.A., and Anderson, D.J. 2001. Expression of ephrinB2 identifies a stable genetic difference between arterial and venous vascular smooth muscle as well as endothelial cells, and marks subsets of microvessels at sites of adult neovascularization. *Dev. Biol.* **230:** 139–150.

Tanaka, M., Kamo, T., Ota, S., and Sugimura, H. 2003. Association of Dishevelled with Eph tyrosine kinase receptor and ephrin mediates cell repulsion. *EMBO J.* **22:** 847–858.

Terashima, A., Cotton, L., Dev, K.K., Meyer, G., Zaman, S., Duprat, F., Henley, J.M., Collingridge, G.L., and Isaac, J.T. 2004. Regulation of synaptic strength and AMPA receptor subunit composition by PICK1. *J. Neurosci.* **24:** 5381–5390.

Thurston, G. 2003. Role of Angiopoietins and Tie receptor tyrosine kinases in angiogenesis and lymphangiogenesis. *Cell Tissue Res.* **314:** 61–68.

Veikkola, T., Jussila, L., Mäkinen, T., Karpanen, T., Jeltsch, M., Petrova, T.V., Kubo, H., Thurston, G., McDonald, D.M., Achen, M.G., et al. 2001. Signalling via vascular endothelial growth factor receptor-3 is sufficient for lymphangiogenesis in transgenic mice. *EMBO J.* **20:** 1223–1231.

Wang, H.U., Chen, Z.F., and Anderson, D.J. 1998. Molecular distinction and angiogenic interaction between embryonic arteries and veins revealed by ephrin-B2 and its receptor Eph-B4. *Cell* **93:** 741–753.

Wigle, J.T. and Oliver, G. 1999. Prox1 function is required for the development of the murine lymphatic system. *Cell* **98:** 769–778.

Wigle, J.T., Harvey, N., Detmar, M., Lagutina, I., Grosveld, G., Gunn, M.D., Jackson, D.G., and Oliver, G. 2002. An essential role for Prox1 in the induction of the lymphatic endothelial cell phenotype. *EMBO J.* **21:** 1505–1513.

Yuan, L., Moyon, D., Pardanaud, L., Breant, C., Karkkainen, M.J., Alitalo, K., and Eichmann, A. 2002. Abnormal lymphatic vessel development in neuropilin 2 mutant mice. *Development* **129:** 4797–4806.

Zimmer, M., Palmer, A., Kohler, J., and Klein, R. 2003. EphB–ephrinB bi-directional endocytosis terminates adhesion allowing contact mediated repulsion. *Nat. Cell Biol.* **5:** 869–878.

Zimmermann, P., Meerschaert, K., Reekmans, G., Leenaerts, I., Small, J.V., Vandekerckhove, J., David, G., and Gettemans, J. 2002. PIP(2)–PDZ domain binding controls the association of syntenin with the plasma membrane. *Mol. Cell* **9:** 1215–1225.